ACS APPLIED MATERIALS & INTERFACES

Research Article

www.acsami.org

# Highly Reflective Liquid Mirrors: Exploring the Effects of Localized Surface Plasmon Resonance and the Arrangement of Nanoparticles on Metal Liquid-like Films

Yu-Ting Yen,[†] Tai-Yen Lu,[†] Yang-Chun Lee,[†] Chen-Chieh Yu,[†] Yin-Chih Tsai,[‡] Yi-Chuan Tseng,[†] and Hsuen-Li Chen*[,†]

[†]Department of Materials Science and Engineering, National Taiwan University, No. 1, Sec. 4, Roosevelt Road, Taipei 10617, Taiwan

[‡]Institute of Astronomy and Astrophysics, Academia Sinica, No. 1, Sec. 4, Roosevelt Road, Taipei 10617, Taiwan

**ABSTRACT:** In this paper, we describe a high-reflectance liquid mirror prepared from densely packed silver nanoparticles (AgNPs) of two different sizes. We controlled the particle size during the synthetic process by controlling the temperature. Varying the concentration of the ligand also allowed us to optimize the arrangement of the AgNPs to achieve liquid mirrors exhibiting high specular reflectance. Scanning electron microscopy and atomic force microscopy confirmed that the particles of the liquid mirror were well-packed with an interparticle distance of merely 2 nm; thus, the interstices and surface roughness of the NPs were effectively minimized. As a result of decreased scattering loss, the reflectance in the shorter wavelength regime was increased effectively. The AgNP film was also sufficiently thick to reflect the light in the longer wavelength regime. In addition, we used three-dimensional finite-difference time domain simulations and experimental measurements to investigate the relationship between the localized surface plasmon resonance (LSPR) and the specular reflection of the liquid mirrors. By changing the packing density of the AgNPs, we found that the LSPR effect could yield either a specular reflection peak or dip at the LSPR wavelengths in the reflection spectra of the liquid mirrors. Relative to previously reported liquid mirrors, the reflectance of our system is obviously much greater, especially in the shorter wavelength regime. The average reflectance in the range from 400 to 1000 nm could reach 77%, comparable with that of mercury-based liquid mirrors.

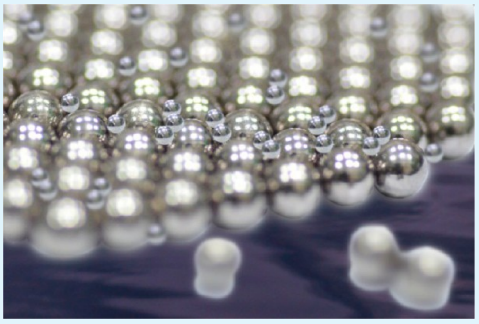

**KEYWORDS:** *liquid mirror, nanoparticles, localized surface plasmon resonance (LSPR), specular reflection, metal liquid-like films*

## INTRODUCTION

Mankind has been interested in astronomy for a long time. To meet the needs of more accurate observations and increased measurement of incident light, the apertures of mirrors used in telescopes must be extremely large. Traditionally, astronomical optical devices are made from glass, which can be difficult and expensive to polish and difficult to fabricate into optical surfaces with parabolic shapes.

Mercury (Hg) is the first material used for the preparation of liquid mirrors because of its high reflectivity and low melting point. Being a liquid at room temperature, Hg can be used to fabricate rotating liquids that satisfy the requirements of surfaces with deformability and high reflectivity. Since first being mentioned by Capocci, liquid Hg has been used in the primary mirrors of telescopes. There are, however, some inevitable shortcomings that limit the use of Hg as a liquid mirror for astronomy.[1,2] The high density of Hg hinders its storage stability within telescopes, where it might penetrate to the bottom of the mirror base. Its toxicity is also a serious problem.[3] Furthermore, Hg cannot be used as the mirror of a telescope on the Moon because it would evaporate quickly when exposed to the lunar vacuum.[4]

To overcome these problems, metal liquid-like films (MELLFs) were introduced by Yogev and Efrima for use in astronomical optics.[5−9] When they added a reducing agent into a chloroform or dichloroethane solution containing silver nitrate and anisic acid, they observed a reflective metallic particle film forming at the water−organic solvent interface. Subsequently, Gordon et al. prepared MELLFs through an alternate synthetic route;[10] adding some ligands to a silver (Ag) colloid, they found that silver nanoparticles (AgNPs) could be extracted at the water−organic solvent interface to form a reflective MELLF. Although these two methods are similar, they differ in that the AgNPs are extracted by the ligand in the latter method, such that the MELLF is not only defined at the liquid phase interface but also readily transferred to the surface of an aqueous or other solution for a specific application. Accordingly, most practitioners prefer preparing MELLFs using Gordon's method.[10]

Unlike other self-assembled NP films formed at liquid interfaces,[11−13] MELLFs display relatively high reflectance.

**Received:** December 30, 2013
**Accepted:** February 27, 2014
**Published:** March 12, 2014

  

Accordingly, Borra et al. applied MELLFs as the mirrors in astronomical optics.[14] Because they are inexpensive, easy to produce, flexible on nonplanar bases, and can be prepared on large scales, MELLFs appear to be suitable replacements for Hg-based liquid mirrors. Furthermore, the liquid-like properties of MELLFs allow their optical mirrors to be formed with any particular surface profile while retaining high reflectivity. Thus, Borra et al. suggested that MELLFs could be called "liquid mirrors." They also demonstrated that MELLFs retained their high reflectivity after being transferred onto paraffin oil surfaces, and that they can be transferred onto some ferrofluids with characteristics necessary for the stability of telescopes on the Moon.[15,16]

If we are to use such liquid mirrors as astronomical optics, it will be necessary to enhance their reflectance. A major parameter that influences the reflectance of a liquid mirror is the MELLF's surface morphology, which depends on the size and arrangement of the NPs. Therefore, to increase the reflectance of liquid mirrors, we must develop methods for controlling the particle size and optimizing their assembly. In past studies, several methods have been employed to control the sizes of AgNPs, including changing the concentration of sodium citrate and the reaction temperature.[17−21] By varying the synthetic temperature, Borra et al. controlled the sizes of NPs and studied their influence on the reflectance of liquid mirrors.[3,14] In the short wavelength regime, the reflectance of a liquid mirror comprising stacks of larger NPs was lower than that of stacks of smaller particles, due to the scattering effect and dissipative absorption. Notably, however, the limitations of the ligand have made it difficult to fabricate continuous, interstitial-free, multilayered NP films.[22] Liquid mirrors consisting of continuous NP films have almost always been monolayers; therefore, the thickness of the liquid mirror has merely been equal to the NP size. As a result, the reflectance of a liquid mirror comprising small NPs will be lower than that of one comprising large NPs. Therefore, to increase the reflectance of liquid mirrors over a broad wavelength regime, it will be necessary to decrease scattering effects while increasing the effective thickness. Another parameter that might influence the reflectance of liquid mirrors is the arrangement of the AgNPs. Generally, increasing the ligand concentration will increase the reflectance of a liquid mirror, because the ligand would also adjust the arrangement of the AgNPs. Although optimizing the ligand concentration can help to bring the AgNPs close enough together to increase the degree of packing, the highest average reflectance previously reported for liquid mirrors at wavelengths in the range from 400 to 1000 nm has been only 69%; that is, approximately 92% of the reflectance of Hg.[23]

Recently, the reflectance of gold (Au) liquid mirror has been discussed by Girault et al.[24] They injected 60 nm gold nanoparticles (AuNPs) onto oil/water interface and studied the reflectance and conductance of AuNP films. However, due to the inherent characteristic of metals, the reflection of Au in the visible regime is lower than that of Ag. Moreover, the AuNPs in the mirror were not captured by chemical ligands; there were many vacancies between AuNPs. As a result, even though the AuNPs already formed a near monolayer of NP film, the average reflectance on the AuNP mirror system was only ca. 10%. In this study, to improve the quality and reflectance of liquid mirrors, we developed a convenient and practical approach to prepare liquid mirror films stacked with NPs of various sizes. We found that when the liquid mirror comprised merely large particles, the surface would be relatively rough, with many interstices between each pair of NPs. Therefore, we introduced small NPs into the synthetic procedure. That is, we mixed solutions of large and small NPs, letting the smaller particles fill the interstices.

In addition to the reflection behavior of AgNPs on liquid mirrors, the localized surface plasmon resonance (LSPR) effect of the NPs at liquid−liquid interfaces has been explored.[25−28] But the simulations in these studies did not considered the condition of the most closely packed NP films. Here, we discussed the relationship between the LSPR effect of the NPs and the specular reflection of the closely packed liquid mirrors. LSPR properties make these self-assembled NP films capable of being plasmonic devices. Some applications have been investigated for photocatalysis[29] and use as surface enhanced Raman scattering (SERS) substrates.[30−32] Besides, we optimized the ligand concentration to ensure that the NPs were packed densely. By minimizing the interstices, the surfaces of the AgNP-based liquid mirrors became flatter, which helped to increase the specular reflectance, especially in the shorter wavelength regime. Moreover, a liquid mirror comprising large and small AgNPs could be sufficiently thick to reflect light at longer wavelengths. Therefore, the reflectances of the liquid mirrors prepared in this study were significantly greater than those reported previously.[23]

## RESULTS AND DISCUSSION

Figure 1 displays a schematic representation of the procedures used for the preparation of the liquid mirrors. To prepare the self-assembled AgNP-based liquid mirror, a chemical reduction method was adapted, with the volume ratio of the $AgNO_3$ solution to the sodium citrate solution selected at 20:1.[10] A

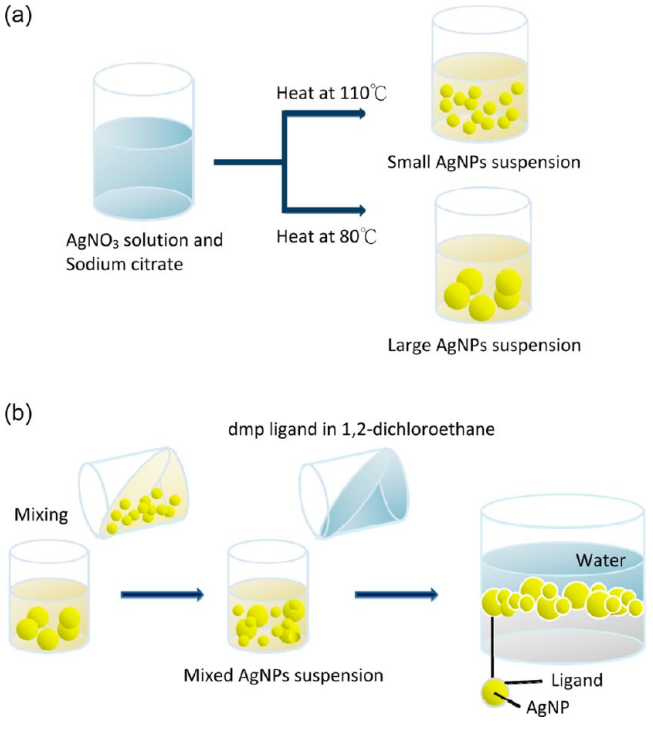


**Figure 1.** Schematic representations of (a) the synthesis of AgNPs of different sizes by heating the reaction solution at different temperatures and (b) the mixing of colloidal solutions of large and small AgNPs to form a liquid mirror.

mixture of 100 mM aqueous $AgNO_3$ (20 mL) and 1% aqueous sodium citrate (5 mL) was heated for 30 min while stirring. Among the several means of controlling the AgNP diameters during the reduction procedure, in this study it was controlled by varying the reaction temperature. Reaction temperatures of 110 and 80 °C provided the large and small AgNPs, respectively. When the reaction temperature was 110 °C, the nucleation rate of the reduced particles was fast, resulting in a high density of small AgNPs. In contrast, synthesis at a lower temperature of 80 °C resulted in large AgNPs. During the synthesis process, the color of the solution changed gradually from transparent and light yellow to pale brown as a result of the LSPR effect of the AgNPs.

After preparing colloidal solutions containing AgNPs of different sizes, 1 mM 2,9-dimethyl-1,10-phenanthroline (dmp) in 1,2-dichloroethane was mixed with each colloidal solution with intense shaking to ensure that dmp monolayers uniformly covered the surfaces of the AgNPs. Different ligand concentrations were tested to explore the influence of the ligand density on the arrangement of the particles. According to the principle of "like dissolves like," the ligand-covered AgNPs resided at the water−dichloroethane interface to form highly reflective AgNP films (Figure 1). After removing the water and the organic layer, the liquid mirror layer could be readily poured onto a water or alcohol solution, a glass or silicon wafer, or even a flexible substrate (e.g., filter paper) to form flat, highly reflective plates.

According to previous studies, liquid mirrors prepared from monodisperse AgNPs face the problem that they cannot satisfy the requirement of high reflection over a broad bandwidth.[14] Using larger AgNPs to prepare liquid mirrors can increase the reflection at longer wavelengths, but the greater surface roughness of these AgNPs would seriously decrease the specular reflection in the shorter wavelength regime.[14] Light scattering and reflective behavior are highly relative to the wavelength of the incident light and the size of the particles. The scattering cross-section of a particle is proportional to its radius.[33,34] If liquid mirror composes of only large NPs, the surface roughness would be higher than that composed of small NPs. The incident light in longer wavelength region would be reflected by the NPs film, but strong scattering would happen in the shorter wavelength region. Moreover, liquid mirrors consisting of continuous NP films are almost always monolayers, meaning that the thickness of the liquid mirror is merely equal to the dimensions of the NPs.[22] When liquid mirrors composed of only small NPs, the scattering effect could be effectively decreased as surface roughness decreased. But the film thickness would be insufficient to reflect the light in longer wavelength region. If we wish to increase the reflectance of liquid mirrors over the whole spectral range and thereby improve their applicability, we would have to find a way to stack NPs into liquid mirrors having relatively flat surfaces and sufficient thickness, while decreased scattering effects. First, we tested the effect of mixing AgNPs of various sizes, prepared by varying the synthetic temperature. Our strategy was to mix the large and small AgNPs, such that the smaller particles would fill the interstices between the larger ones, providing flatter liquid mirror films that would retain the thickness of a monolayer comprising the larger particles.

Figure 2 displays the normalized absorption spectrum of a colloidal solution synthesized at 80 °C. The spectrum features an absorption peak at 480 nm, representing the LSPR of the AgNPs. This absorption peak blue-shifted to 414 nm for the

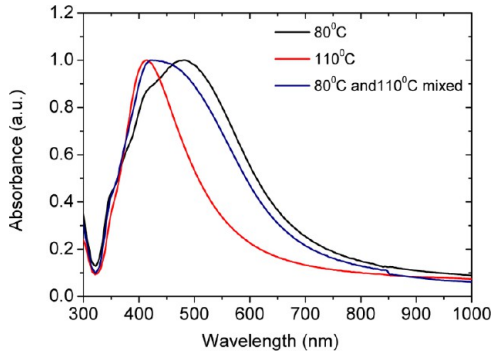


**Figure 2.** Absorption spectra of the AgNP colloids synthesized at 80 °C (black line) and 110 °C (red line) and of a mixture of these colloid solutions at a volume ratio of 3:1 (blue line).

AgNPs synthesized at 110 °C. According to previous reports, the absorption peaks of larger NPs are red-shifted relative to those of smaller NPs. Therefore, the NPs synthesized at 80 °C were larger than those prepared at 110 °C. Next, we directly mixed the colloid solutions containing each type of AgNPs to obtain a mixture of large and small particles. As displayed in Figure 2, a 3:1 volume ratio of the colloidal solutions of the larger and smaller NPs provided a normalized absorption peak for the mixed suspension that was between those of the original two solutions; it appeared at 430 nm and was broader than either of the individual signals. This phenomenon arose from the absorption peak of the smaller NPs being at a shorter wavelength with respect to that of the larger particles, meaning that the absorption peak of the NP mixture would exhibit the LSPR phenomena of the different sized NPs, resulting in a broader absorption band.

To investigate the surface morphologies of liquid mirrors, we transferred the AgNP-based liquid mirrors onto silicon wafer substrates. Images a and b in Figure 3 display SEM images of liquid mirrors assembled from the AgNPs that had been formed at 80 and 110 °C, respectively; corresponding particle-size distributions are displayed at the bottom of each image. In Figure 3a, we found that the liquid mirror comprised AgNPs having a diameter of approximately 100 nm; they were not closely packed, resulting in many spaces between the individual AgNPs. In Figure 3b, the AgNPs synthesized at higher temperature possessed a particle size of approximately 50 nm; the surface of this liquid mirror was relatively densely packed. Moreover, Figure 3c displays an SEM image of the liquid mirror prepared from the mixture of AgNPs of various sizes; it comprised both the larger (diameter: ca. 100 nm) and smaller (diameter: ca. 50 nm) AgNPs, with two primary peaks in the size distribution. The gaps between the large AgNPs were minimized because the small NPs were situated within these gaps. From these images, the mixing of the large and small AgNPs appeared to decrease the surface roughness while increasing the effective thickness of the AgNP-based liquid mirror, suggesting that it might exhibit high specular reflectance over a broad bandwidth.

Next, we used AFM to investigate the relationship between the surface roughness and the reflectance of the liquid mirror. We transferred the liquid mirror from the water−air interface onto a glass substrate to perform these observations. Images a and b in Figure 4 display AFM images of the liquid mirrors comprising the large AgNPs and the mixed AgNPs, respectively. The AFM image in Figure 4a revealed that the

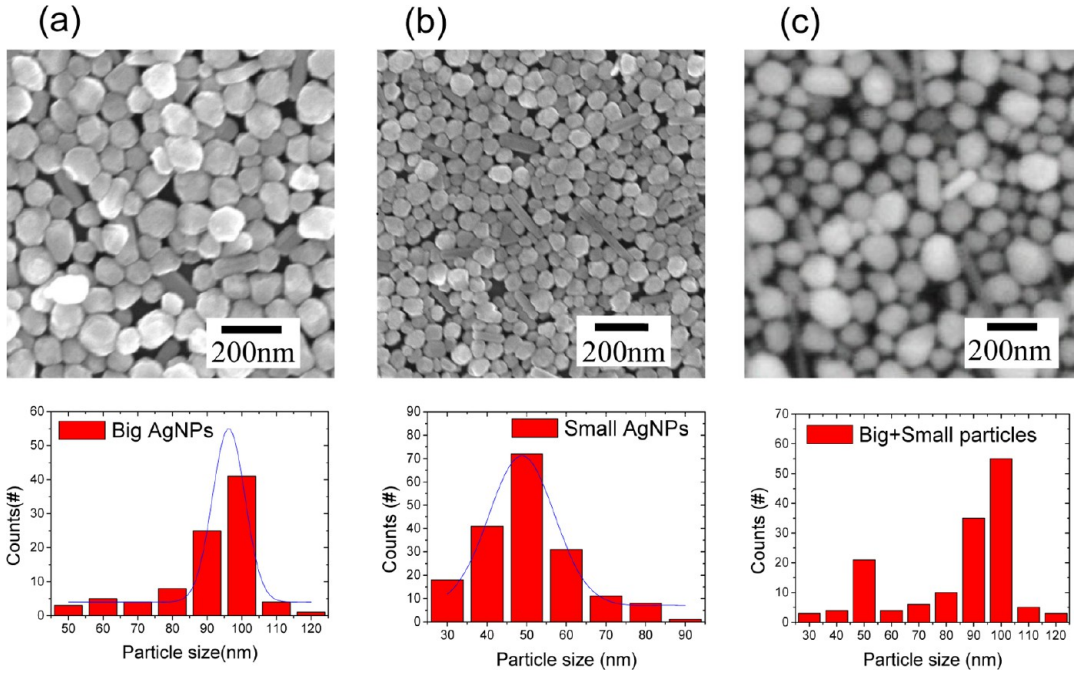


**Figure 3.** SEM images and particle size distribution diagrams of (a) the large AgNPs (ca. 100 nm), (b) the small AgNPs (ca. 50 nm), and (c) the mixture of the large and small AgNPs.

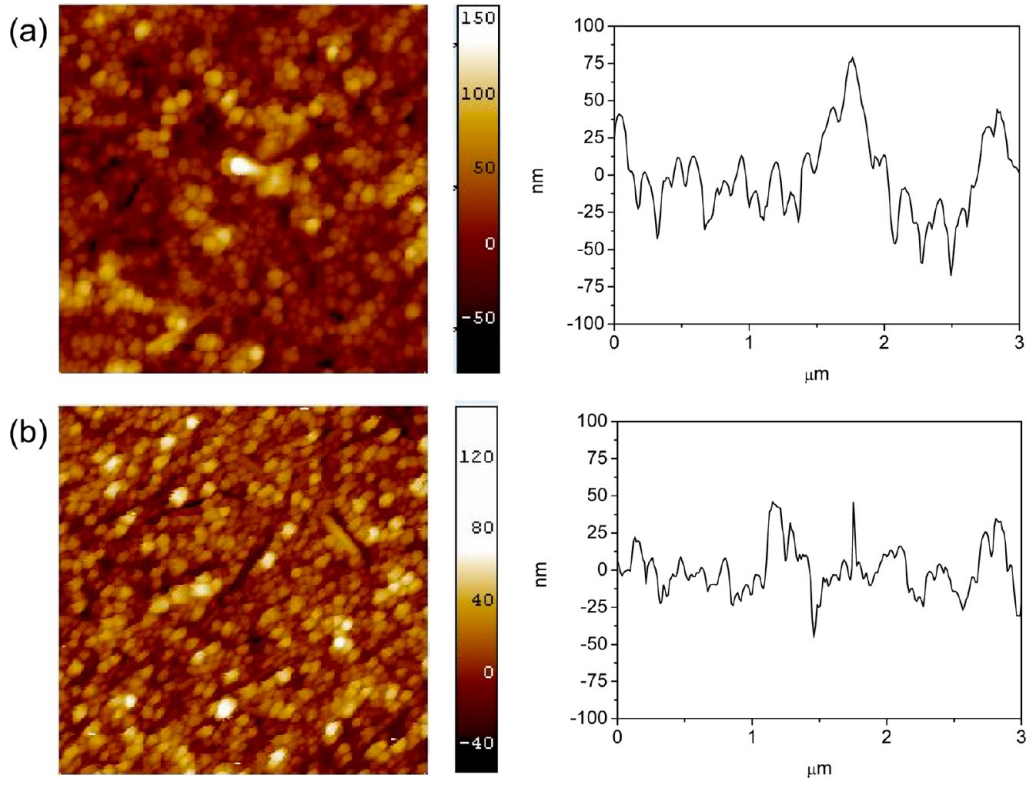


**Figure 4.** AFM images and cross-sectional analyses of liquid mirrors comprising (a) the large AgNPs and (b) the mixture of large and small AgNPs, prepared at a dmp concentration of 0.005 M.

surface was relatively rough when the liquid mirror comprised AgNPs having a diameter of approximately 100 nm. The cross-sectional analysis provided a root-mean-square surface roughness of approximately 16 nm, suggesting that this mirror might exhibit low reflectance. On the other hand, the root-mean-square roughness of the surface of the mixed AgNPs (Figure 4b) was less than 10 nm, because the small AgNPs filled the gaps between the large particles, suggesting that the reflectance would be enhanced effectively. The smaller NPs would also assist in decreasing the interparticle spacing further if the arrangement of AgNPs were to be improved by varying the concentration of the ligand.


dx.doi.org/10.1021/am406048s | ACS Appl. Mater. Interfaces 2014, 6, 4292−4300

To examine the quality of our various liquid mirrors, we measured their reflectance using a reflectometry system. The reflectometry provided a white light source through an optical fiber. The fiber was set to be vertically above on liquid mirrors at an incident angle of 0° and the reflection light was collected at the same time. In addition, we also measured the reflectance of the preknown reflectance substrates, such as silicon wafer or glass, under the same optical setup to examine the absolute reflectance of our liquid mirrors. The reflectance spectra were all derived in liquid state of AgNP films, without transferred onto solid substrates. As displayed in Figure 5a, the reflectance

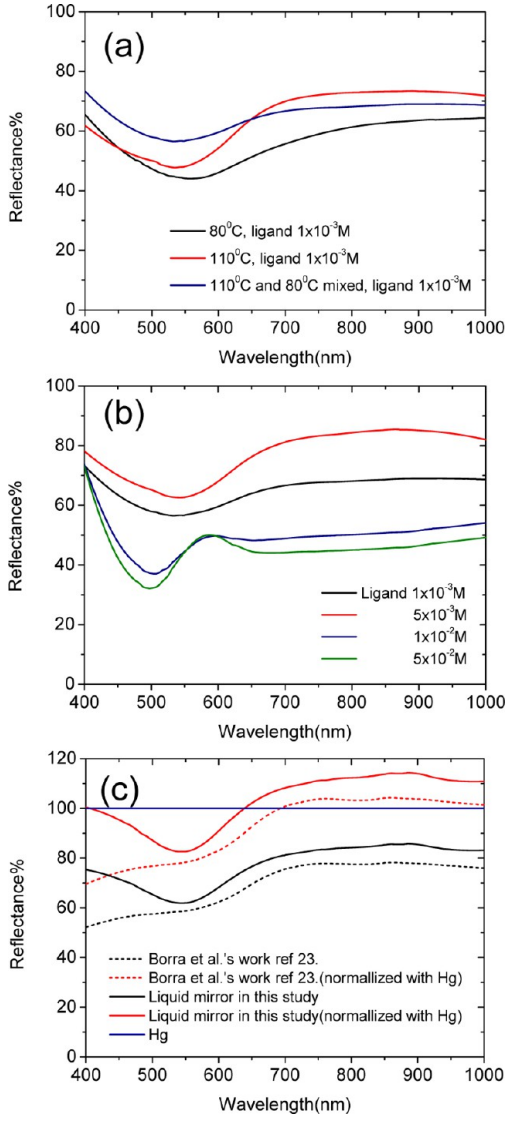


**Figure 5.** (a, b) Reflectance spectra of liquid mirrors comprising (a) large (black line), small (red line), and mixed (blue line) AgNPs and (b) mixed AgNPs prepared at different dmp ligand concentrations. (c) Reflectance spectra of the liquid mirrors in this study compared with the best results from a previous report, both normalized to Hg.

of the liquid mirror comprising the larger AgNPs was lower than that of the liquid mirror comprising the smaller AgNPs. The lowest reflectance of the mirror comprising the large AgNPs was 43% at a wavelength of 550 nm; the reflectance in the longer wavelength region was approximately 60%. On the other hand, the reflectance dip of the smaller AgNP-based liquid mirror was 45% at a wavelength of 525 nm, reaching approximately 70% in the longer wavelength region. We attribute the lower reflectance of the liquid mirror prepared from the larger AgNPs over the whole wavelength range to the lower density of the packing of these large NPs, as observed in Figure 3a. To optimize the surface roughness of the liquid mirror, we mixed the colloidal solutions of the large and small AgNPs at a volume ratio of 3:1, such that the smaller AgNPs would fill the interstices to form a liquid mirror having a flatter, more-continuous surface. As displayed in Figure 5a, the reflectance dip of the mixed liquid mirror increased significantly to approximately 55% at a wavelength of 530 nm. The average reflectance in the longer wavelength region was approximately 68%, slightly lower than that of the liquid mirror comprising only smaller AgNPs. We suspect that although the smaller AgNPs filled the gaps between the pairs of individual larger AgNPs, the arrangement of the mixed AgNPs would require further optimization to obtain a liquid mirror exhibiting higher reflectance.

Because we formed the liquid mirrors after extracting the AgNPs from a colloidal solution of the ligand dmp, we suspected that the concentration of dmp would certainly influence the arrangement of the particles during the process. Indeed, a previous study revealed that the reflectance could be improved by varying the concentration of dmp.[22] To further increase the reflectance of our liquid mirror comprising a mixture of both large and small AgNPs, we tested the effects of dmp concentrations from 0.001 to 0.05 M on the reflectance of the resulting liquid mirrors; Figure 5(b) presents the corresponding reflectance spectra. We observe that the reflectance of the liquid mirror increased upon increasing the dmp concentration from $1 \times 10^{-3}$ to $5 \times 10^{-3}$ M; the measured reflectance increased from 55 to 60% at 550 nm and from 69 to 84% in the longer wavelength regime, with the average reflectance increasing from 65 to 77%. Any further increase in the dmp concentration caused the reflectance to decrease. We attribute this phenomenon to the aggregation of the ligand, such that it could not effectively cover the surfaces of the AgNPs, resulting in a gradual greater difficulty in the formation of the liquid mirrors. In other words, when the ligand concentration was greater than $5 \times 10^{-3}$ M, increasing the concentration of ligand did not improve the reflectance of the liquid mirror.

Next, we compared the reflectance of our liquid mirror prepared using the mixed AgNPs with that of the best result reported by Borra et al.[23] Figure 5c displays the absolute reflectance and relative reflectance, normalized to Hg, for both liquid mirrors. Gratifying, the average reflectance at wavelengths ranging from 550 to 1000 nm increased from 74 to 80% (from 96 to 104%, normalized to Hg); in the shorter wavelength regime (from 400 to 550 nm), it increased significantly from 56 to 68% (from 73 to 88%, normalized to Hg). Most of the increase in reflectance was contributed from the short wavelength regime (blue light) because the lower surface roughness of the liquid mirror film greatly decreased the associated scattering loss.

The reflectance spectra in Figures 4 and 5 feature obvious reflection dips. To investigate their origin, we considered the relationships between the arrangement of the AgNPs and the resulting specular reflection of the liquid mirrors. In the LSPR phenomenon, the conduction electron cloud of the metal NPs will oscillate with the electric field of the incident light. As a result, the electric field between pairs of NPs at specific spots

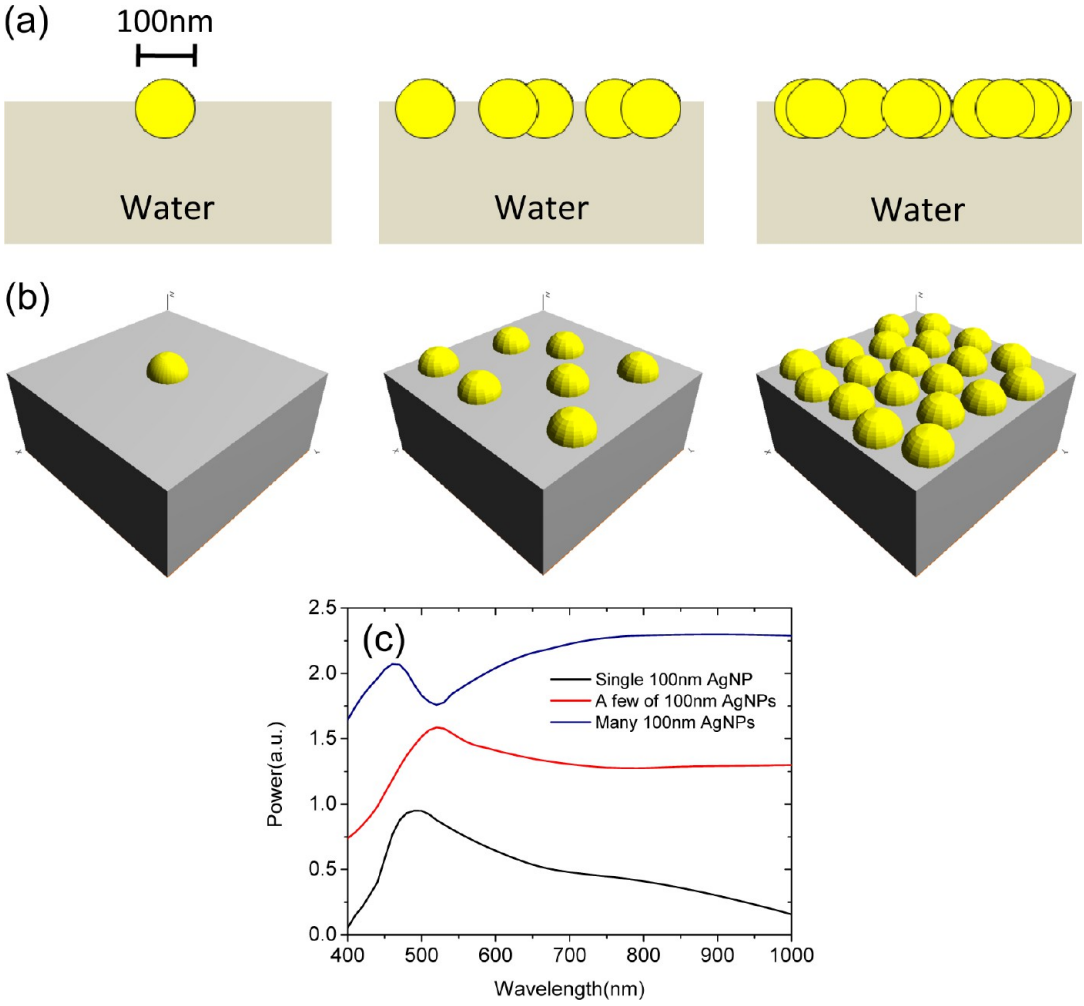


**Figure 6.** (a, b) Schematic representations of the setups for 3D-FDTD simulations of (from left to right) a single AgNP, a few AgNPs, and many AgNPs, each positioned on a water surface. These simulations were conducted using randomly distributed AgNPs having a diameter of 100 nm. (c) FDTD-simulated specular reflection power of the liquid mirrors.

would be enhanced. This phenomenon is called the particle plasmon or localized surface plasmon.[35] Thus, the particle sizes, densities, and shapes influenced the resonance wavelengths in the spectra. We performed 3D-FDTD simulations to investigate the relationships between the specular reflection of the liquid mirrors and the arrangements of their AgNPs. Panel a and b in Figure 6 reveal the simulation setups for NPs having a diameter of 100 nm in various arrangements: a single AgNP, a few AgNPs, and closely packed AgNPs on the water surface. The detector was set over 4 $\mu$m above the water surface to better represent the specular reflection. Figure 6c displays the simulation data. For a single AgNP, the reflection peak appeared near 500 nm, which is the LSPR wavelength of a single AgNP. As the number of AgNPs increased, a coupling effect occurred between the NPs, causing the peak to red-shift slightly to 520 nm and the reflective power to increase in the longer wavelength region. Finally, when numerous closely packed AgNPs were present, almost forming a continuous NP film, the reflective power increased further in the longer wavelength region; we found, however, that a reflection dip appeared at a wavelength of approximately 520 nm. We suspect that these phenomena originated from the extinction phenomenon of the LSPR on the AgNPs. The extinction from the LSPR effect contained both absorption and scattering effects. Because the extinction was quite strong at the wavelength of the LSPR, the scattering that occurred in all directions was strong as well. This strong scattering presumably contributed to the specular reflection because it occurred in the direction that agreed with reflection. Thus, the resulting increased specular reflection would be improved if only a single AgNP or a few AgNPs existed on the water surface. In contrast, the reflectance away from the characteristic LSPR wavelength was caused merely by common surface reflection; therefore, it would not be enhanced. If there were abundant AgNPs that formed a continuous film, however, the NP film would be quite flat. The specular reflection itself was sufficiently high when the contribution from the backscattering of the LSPR effect was not evident. Here, the absorption term of the LSPR effect was dominant over the specular reflection at the resonating wavelength that caused the dip in the reflectance spectrum. As a result, except at the LSPR wavelength, the reflectance was rather high over a broad wavelength regime, as the measured data confirmed in Figure 5.

To further investigate the relationship between the reflectance and the surface roughness of the liquid mirror, we also used the 3D-FDTD method to simulate the reflectance of liquid mirrors possessing different surface morphologies. Figure 7 displays schematic representations of the simulation setup. In

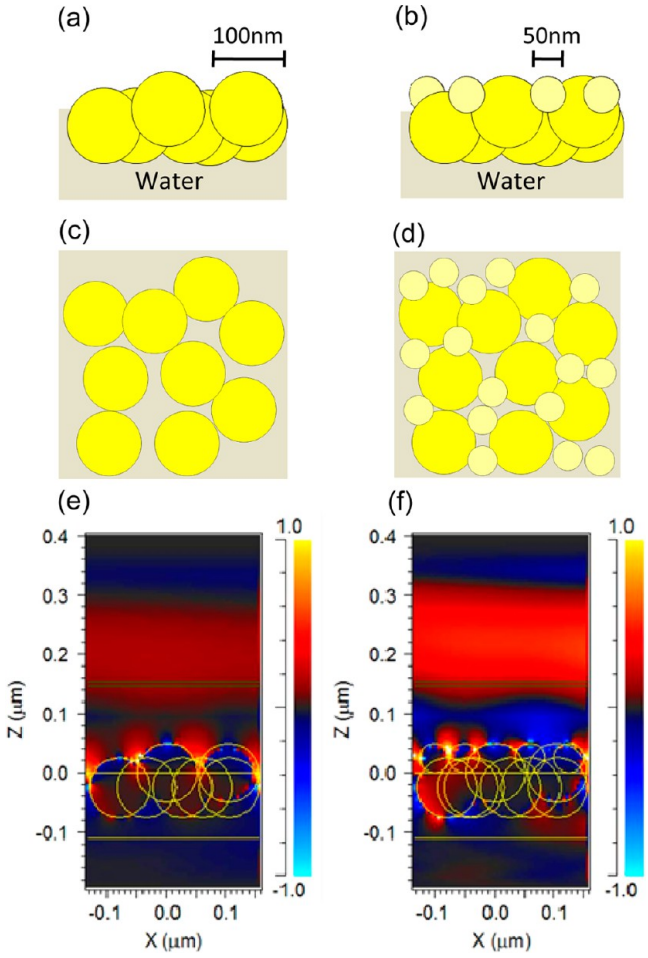


**Figure 7.** (a–d) Schematic representations of the setups of 3D-FDTD simulations and (e, f) FDTD simulations of the electric field distributions of a plane waves (wavelength: 400 nm) propagating onto liquid mirrors comprising (a, c, e) randomly distributed AgNPs (diameter: 100 nm) and (b, d, f) a randomly distributed mixture of large and small AgNPs (diameters: 100 and 50 nm, respectively).

panels a and c in Figure 7, we used a model of a liquid mirror comprising only 100 nm AgNPs distributed randomly at the air–water interface. In panels b and d in Figure 7, the simulation model featured many 100 nm AgNPs surrounded by 50 nm AgNPs in their interparticle spaces; in accord with the SEM image, we set the gaps between each pair of NPs to be 2 nm. We measured the simulated reflectance electric field distributions of a plane wave featuring a wavelength of 400 nm propagating into these two kinds of liquid mirrors. From Figure 7e, we calculated the reflectance of the liquid mirror based on randomly distributed large AgNPs to be approximately 30% at 400 nm. After the 50 nm AgNPs had been introduced into the system, Figure 7f reveals that the reflectance in shorter wavelength region had been increased effectively. It was evident that the simulated reflectance at 400 nm rose to approximately 55%, due to the improvement in average surface flatness after filling the smaller particles into the interstices between the larger particles. Although we could set up our simulations with only spherical AgNPs, because of the inherent limitations of FDTD simulation settings, not all of the particles in the liquid mirror were spherical—there were also some polygonal AgNPs, as revealed in the SEM images in Figure 5a. It was evident in the SEM images that the non-spherical particles filled the interstices better than the spherical ones did, forming a much more continuous and flatter liquid mirror surface. The measured reflectance of the liquid mirror was slightly better than the conditions we used in our simulations. According to the simulation data, we conclude that the reflectance of a liquid mirror in the shorter wavelength regime is influenced largely by its surface roughness.

Figure 8 displays photographic images of the liquid mirrors prepared in this study. In Figure 8a, a specular reflecting image

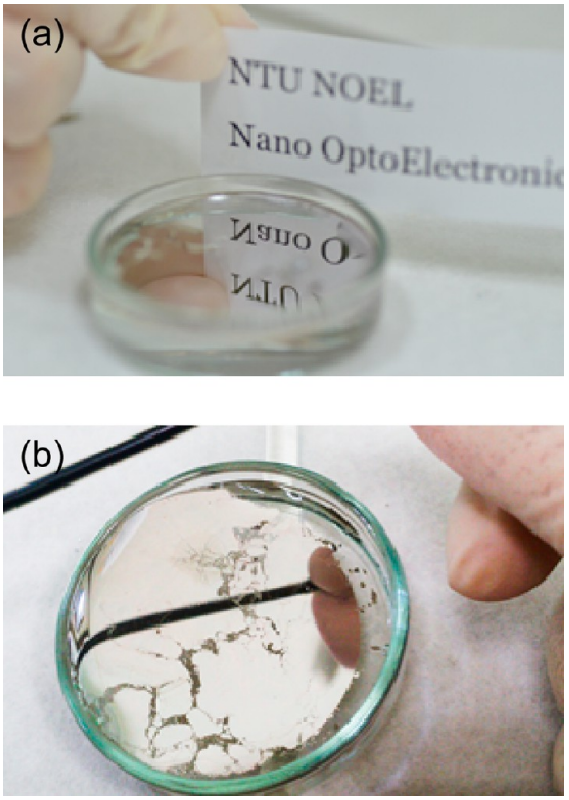


**Figure 8.** Photographic images of (a) the highly reflective liquid mirror and (b) the deformability of the liquid mirror.

is clearly evident in the liquid mirror, which was highly reflective because of its relatively flat surface. Moreover, Figure 8b demonstrates one of the most important qualities of a liquid mirror: its deformability. In this case, we used a glass rod to tilt the Petri dish, so that the liquid mirror was nearly overflowing. Because of the surface tension of the water, the liquid mirror acted like a curved reflection surface. In this photograph, we observe the distorted image of a straight ball point pen, reflected by the liquid mirror. This picture reveals that the liquid mirror was readily deformed as a result of its liquid nature.

## CONCLUSIONS

We have prepared a densely packed liquid mirror, exhibiting high specular reflectance, from a mixture of AgNPs having two different diameters. We controlled the particle sizes of these AgNPs by varying the temperature during the synthetic process. We also optimized the ligand concentration, which influenced the arrangement of the AgNPs, to optimize the high reflectance of the liquid mirrors. We mixed colloidal solutions of the large and small AgNPs at a volume ratio of 3:1, with the concentration of ligand optimized at 0.005 M. SEM images

confirmed that the particles in the liquid mirror were well packed as a result of the mixing of the large and small AgNPs. The interparticle distance in the liquid mirror was merely 2 nm as a result of the interstices having been effectively minimized. AFM images revealed that the surface roughness also decreased when combining the large and small AgNPs and optimizing the concentration of the ligand. A decrease in the scattering loss caused the reflectance in the shorter wavelength regime to increase effectively. In addition, the AgNP film was sufficiently thick to reflect light in the longer wavelength regime. Thus, our liquid mirror satisfied both of the requirements—a thick film and a flat surface—for highly reflective properties over a broad wavelength regime. In addition, we used 3D-FDTD simulations and experimental measurements to investigate the relationships between LSPR effects of the AgNPs and the specular reflection of the liquid mirrors. By changing the packing density of the AgNPs, we found that the LSPR effect could yield a specular reflection peak or reflection dip at the LSPR wavelength in the reflection spectra of the liquid mirrors. Comparing our liquid mirror in this study with the best results reported previously, we increased the average reflectance at wavelengths in the range 550−1000 nm from 74 to 80% and that in the range 400−550 nm greatly from 56 to 68%. The average reflectance in the range from 400 to 1000 nm reached 77%, comparable with that of Hg-based liquid mirrors. Its liquidlike properties suggest that this liquid mirror will be suitable for fabricating large-scale mirrors with desired shapes. The deformability of this liquid mirror allows it to be readily transferred onto different kinds of substrates for applications in various devices.

## METHODS

**Chemicals.** Silver nitrite ($AgNO_3$, 99.9999%), neocuproine free base (2,9-dimethyl-1,10-phenanthroline, dmp, ≥98%) and 1,2-dichloroethane (DCE, ≥99.0%) were purchased from Aldrich. Trisodium citrate dihydrate ($Na_3C_6H_5O_7{\cdot}2H_2O$) was purchased from SHOWA. All the chemicals were used as received without further purification. Deionized water (18.2MΩ·cm) was used in all synthesis processes.

**Preparation of AgNPs.** We prepared the AgNPs via a chemical reduction method. A mixture of 100 mM aqueous $AgNO_3$ (20 mL) and 1% aqueous sodium citrate (5 mL) was heated for 30 min while stirring. The AgNP diameters were controlled by varying the reaction temperature. Reaction temperatures of 80 and 110 °C provided the large and small AgNPs. Throughout the synthesis process, the color of the solution changed gradually from transparent and light yellow to pale brown as a result of the LSPR effect of the AgNPs. After the color became totally pale brown, the AgNPs colloid were kept heating at 110 and 80 °C for 30 min to make the NPs stable.

**Preparation of Liquid Mirrors.** To explore the relationship between the 2,9-dimethyl-1,10-phenanthroline (dmp) ligand density and the arrangement of the self-assembled AgNPs film, the concentrations of dmp in 1,2-dichloroethane were varied from $1 \times 10^{-3}$ to $5 \times 10^{-3}$ M. These dmp solutions (10 mL) were mixed with each AgNPs colloidal solution (10 mL) at equal volume ratio (1:1) in a separatory funnel. After 5 min of intensely shaking, the ligand-covered AgNPs would form highly reflective AgNP films resided at the water−dichloroethane interface. After removing the water and the organic layer, the liquid mirror layer could be readily poured onto various substrates.

**Characterization.** Absorbance spectra of AgNPs colloids were measured by UV−vis spectrophotometer (U-4100, Hitachi). Specular reflectance spectra of the self-assembled AgNPs films were measured in solution using thin film reflectometry (NanoCal-2000). To investigate the surface morphology and quality of the AgNP films, each liquid mirror was transferred onto a glass or silicon substrate. After dried at room temperature, these samples were subjected to field emission gun scanning electron microscopy (FEG SEM-NOVA NANO SEM 450) and scanning probe microscope as atomic force microscopy (Veeco Innova SPM).

**Optical Simulations.** To explore the relationship between the specular reflection of a liquid mirror and the arrangement of its AgNPs, we used the three-dimensional finite-difference time domain (3D-FDTD) method to simulate the conditions of the specular reflection. The simulation setup was depicted in panels a and b in Figure 6. Three types of AgNPs arrangements were used. First, a single AgNP was placed on the water surface, and then a few more AgNPs were introduced into the system. Finally, AgNPs were numerous enough to form a continuous NPs film on the water surface. Each AgNP had the diameter of 100 nm and was semi-immersed into the water layer. The minimum distance between AgNPs was set to be 2 nm. A plane wave as the light source was placed to be 500 nm above the water surface. The detector was set to be 4.3$\mu$m far above the water surface to ensure the detector collected the specular reflection light. The perfectly matched layer (PML) boundary conditions were used to assure only the specular reflection light could be collected by the detector.

To investigate the relationship between the specular reflectance and the surface roughness of liquid mirror, we also used the FDTD method to simulate the reflectance of liquid mirrors possessed two different surface morphologies. The first model liquid mirror in the simulation consisted of AgNPs having diameters of 100 nm that randomly distributed at the water surface. Part of these AgNPs were semi-immersed into the water layer, the center of these NPs was set to be at the water surface. Next, 50 nm AgNPs were introduced into the system. The center of these small AgNPs was set to be 25 nm above the water surface so as to reduce the surface roughness of liquid mirror. The gaps between adjacent AgNPs were set at 2 nm according to the SEM images. The light source was set to be a plane wave which resided 100 nm above water surface. The PML boundary conditions were also used in these calculations.

## AUTHOR INFORMATION

### Corresponding Author

*E-mail: hsuenlichen@ntu.edu.tw.

### Notes

The authors declare no competing financial interest.

## ACKNOWLEDGMENTS

We thank the National Science Council, Taiwan, and Chung-Shan Institute of Science and Technology for supporting this study under contracts NSC-100-2628-E-002-031-MY3 and NSC 100-2628-E-002-023-MY2.

## REFERENCES

(1) Gibson, B. K. Liquid Mirror Telescopes: History. *J. R. Astron. Soc. Can.* **1991**, *85*, 158−171.
(2) Wood, R.W. The Mercury Paraboloid as A Reflecting Telescope. *Astrophys. J.* **1909**, *29*, 164−176.
(3) Borra, E. F.; Ritcey, A. M.; Bergamasco, R.; Laird, P.; Gingras, J.; Dallaire, M.; Silva, L. D.; Lelievre, H. Y. Nanoengineered Astronomical Optics. *Astron. Astrophys.* **2004**, *419*, 777−782.
(4) Borra, E. F.; Seddiki, O.; Angel, R.; Eisenstein, D.; Hickson, P.; Seddon, K. R.; Worden, S. P. Deposition of Metal Films on An Ionic Liquid as A Basis for A Lunar Telescope. *Nature* **2007**, *447*, 979−981.
(5) Yogev, D.; Efrima, S. Novel Silver Metal Liquidlike Films. *J. Phys. Chem.* **1988**, *92*, 5754−5760.
(6) Yogev, D.; Efrima, S.; Kafri, O. Study of The Thickness of Liquid Layers by Moire Deflectometry. *Opt. Lett.* **1988**, *13*, 934−936.
(7) Yogev, D.; Deutsch, M.; Efrima, S. Structural Studies of Silver Metal "Liquidlike" Films. *J. Phys. Chem.* **1989**, *93*, 4174−4179.
(8) Yogev, D.; Efrima, S. Chemical Aspects of Silver Metal Liquid-Like Films. *J. Colloid Interface Sci.* **1991**, *147*, 88−97.

(9) Farbman, I.; Efrima, S. Studies of The Structure of Silver Metal Liquidlike Films by UV-Visible Reflectance Spectroscopy. *J. Phys. Chem.* **1992**, *96*, 8469−8473.
(10) Gordon, K. C.; McGarvey, J. J.; Taylor, K. P. Enhanced Raman Scattering from "Liquid Metal" Films Formed from Silver Sols. *J. Phys. Chem.* **1989**, *93*, 6814−6817.
(11) Rao, C. N. R.; Kulkarni, G. U.; Thomas, P. J.; Agrawal, V. V.; Saravanan, P. Films of Metal Nanocrystals Formed at Aqueous-Organic Interfaces. *J. Phys. Chem. B* **2003**, *107*, 7391−7395.
(12) Rao, C. N. R.; Kulkarni, G. U.; Thomas, P. J.; Agrawal, V. V.; Gautam, U. K.; Ghosh, M.; Tumkurkar, U. Use of The Liquid−Liquid Interface for Generating Ultrathin Nanocrystalline Films of Metals, Chalcogenides, and Oides. *J. Colloid Interface Sci.* **2005**, *289*, 305−318.
(13) Wang, L.; Sun, Y.; Che, G.; Li, Z. Self-Assembled Silver Nanoparticle Films at An Air−Liquid Interface and Their Aplications in SERS and Eectrochemistry. *Appl. Surf. Sci.* **2011**, *257*, 7150−7155.
(14) Lelievre, H. Y.; Borra, E. F.; Ritcey, A. M.; Silva, L. V. D. Optical Tests of Nanoengineered Liquid Mirrors. *Appl. Opt.* **2003**, *42*, 1882−1887.
(15) Dery, J. P.; Borra, E. F.; Ritcey, A. M. Ethylene Glycol Based Ferrofluid for The Fabrication of Magnetically Deformable Liquid Mirrors. *Chem. Mater.* **2008**, *20*, 6420−6426.
(16) Borra, E. F. Magnetic Liquid Deformable Mirrors for Astronomical Applications: Active Correction of Optical Aberrations from Lower-Grade Optics and Support System. *Astrophys. J., Suppl. Ser.* **2012**, *201*, 8.
(17) Henglein, A.; Giersig, M. Formation of Colloidal Silver Nanoparticles: Capping Action of Citrate. *J. Phys. Chem. B* **1999**, *103*, 9533−9539.
(18) Pyatenko, A.; Yamaguchi, M.; Suzuki, M. Synthesis of Spherical Silver Nanoparticles with Controllable Sizes in Aqueous Solutions. *J. Phys. Chem. C* **2007**, *111*, 7910−7917.
(19) Pillai, Z. S.; Kamat, P. V. What Factors Control the Size and Shape of Silver Nanoparticles in the Citrate Ion Reduction Method? *J. Phys. Chem. B* **2004**, *108*, 945−951.
(20) Jiang, X. C.; Chen, W. M.; Chen, C. Y.; Xiong, S. X.; Yu, A. B. Role of Temperature in the Growth of Silver Nanoparticles Through a Synergetic Reduction Approach. *Nanoscale Res. Lett.* **2011**, *6*, 32.
(21) Amin, M.; Anwar, F.; Ramzan, M.; Janjua, S. A.; Iqbal, M. A.; Rashid, U. Green Synthesis of Silver Nanoparticles through Reduction with Solanum xanthocarpum L. Berry Extract: Characterization, Antimicrobial and Urease Inhibitory Activities against Helicobacter pylori. *Int. J. Mol. Sci.* **2012**, *13*, 9923−9941.
(22) Faucher, L.; Borra, E. F.; Ritcey, A. M. Use of Thiols as Protecting Ligands in Reflective Surface Films of Silver Nanoparticles. *J. Nanosci. Nanotechnol.* **2008**, *8*, 3900−3908.
(23) Gingras, J.; Dery, J. P.; Lelievre, H. Y.; Borra, E. F.; Ritcey, A. M. Surface Films of Silver Nanoparticles for New Liquid Mirrors. *Colloids Surf,. A* **2006**, *279*, 79−86.
(24) Fang, P.P.; Chen, S.; Deng, H.; Scanlon, M. D.; Gumy, F.; Lee, H. J.; Momotenko, D.; Amstutz, V.; Corté s-Salazar, F.; Pereira, C. M.; Yang, Z.; Girault, H. H. Conductive Gold Nanoparticle Mirrors at Liquid/Liquid Interfaces. *ACS Nano* **2013**, *7*, 9241−9248.
(25) Flatté, M. E.; Kornyshev, A. A.; Urbakh, M. Electrovariable Nanoplasmonics and Self-Assembling Smart Mirrors. *J. Phys. Chem. C* **2010**, *114*, 1735−1747.
(26) Kornyshev, A. A.; Marinescu, M.; Pagetw, J.; Urbakhw, M. Reflection of Light by Metal Nanoparticles at Electrodes. *Phys. Chem. Chem. Phys.* **2012**, *14*, 1850−1859.
(27) Yang, Z.; Chen, S.; Fang, P.; Ren, B.; Girault, H. H.; Tian, Z. LSPR Properties of Metal Nanoparticles Adsorbed at a Liquid−Liquid Interface. *Phys. Chem. Chem. Phys.* **2013**, *15*, 5374−5378.
(28) Turek, V. A.; Cecchini, M. P.; Paget, J.; Kucernak, A. R.; Kornyshev, A. A.; Edel, J. B. Plasmonic Ruler at the Liquid_Liquid Interface. *ACS Nano* **2012**, *6*, 7789−7799.
(29) Schaming, D. H.; Hojeij, M.; Younan, N.; Nagatani, H.; Lee, H. J.; Girault, H. H. Photocurrents at Polarized Liquid/Liquid Interfaces Enhanced by a Gold Nanoparticle Film. *Phys. Chem. Chem. Phys.* **2011**, *13*, 17704−17711.
(30) Cecchini, M. P.; Turek, V. A.; Paget, J.; Kornyshev, A. A.; Edel, J. B. Self-Assembled Nanoparticle Arrays for Multiphase Trace Analyte Detection. *Nat. Mater.* **2013**, *12*, 165−171.
(31) Edel, J. B.; Kornyshev, A. A.; Urbakhw, M. Self-Assembly of Nanoparticle Arrays for Use as Mirrors, Sensors, and Antennas. *ACS Nano* **2013**, *7*, 9526−9532.
(32) Konrad, M. P.; Doherty, A. P.; Bell, S. E. J. Stable and Uniform SERS Signals from Self-Assembled Two-Dimensional Interfacial Arrays of Optically Coupled Ag Nanoparticles. *Anal.Chem.* **2013**, *85*, 6783−67895.
(33) Mie, G. Beiträge zur Optik trüber Medien, Speziell Kolloidaler Metallösungen. *Ann. Phys.* **1908**, *25*, 377−445.
(34) Hulst, H. C. *Light Scattering by Small Particles*; Dover Publications: New York, 1981.
(35) Kelly, K. L.; Coronado, E.; Zhao, L. L.; Schatz, G. C. The Optical Properties of Metal Nanoparticles: The Influence of Size, Shape, and Dielectric Environment. *J. Phys. Chem. B* **2003**, *107*, 668−677.